Identification of Aberrant Plasma Exosomal Derived ceRNA Networks in Adolescent with Major Depressive Disorder

Zhifen Liu (zhifenliu@sxmu.edu.cn)
the First Hospital of Shanxi Medical University https://orcid.org/0000-0003-0782-4195
Yifan Xu
the First Hospital of Shanxi Medical University
Rong Zhang
the First Hospital of Shanxi Medical University
Xinzhe Du
the First Hospital of Shanxi Medical University
Yangxi Huang
the First Hospital of Shanxi Medical University
Yao Gao
Yujiao Wen
the First Hospital of Shanxi Medical University
Dan Qiao
Ning Sun

Article

Keywords: Exosome, ceRNA network, Adolescent, Major Depression Disorder

Posted Date: August 14th, 2023

DOI: https://doi.org/10.21203/rs.3.rs-2348047/v5

Abstract

Major Depressive Disorder (MDD) during adolescence significantly jeopardizes both mental and physical well-being. However, the etiology underlying MDD in adolescents remains unclear. Our study enrolled a total of 114 adolescent participants who underwent comprehensive clinical and cognitive assessments. Differential expressions of long non-coding RNAs (lncRNAs) and messenger RNAs (mRNAs) within plasma exosomes were determined through microarray analysis. A total of 3752 dysregulated lncRNAs and 1789 dysregulated mRNAs were identified. Subsequently, two distinct sets of competitive endogenous RNA (ceRNA) networks were established. The candidate regulatory axes (AC156455.1/miR126-5p/AAK1 and CCDC18AS1/miR6835-5p/CCND2) were chosen from the ceRNA networks and subsequently validated within the cohort using quantitative real-time polymerase chain reaction (qRT-PCR). Our findings reveal that the candidate regulatory axes exhibit diverse expression patterns among both adolescents with MDD and healthy controls (HCs), both prior to and post-treatment in adolescents with MDD. Furthermore, the expression levels of AAK1, CCDC18AS1, and miR6835-5p exhibited significant differences between the response and non-response groups. Baseline expression level of CCDC18-AS1, miR-6835-5p and CCND2 could predict the therapeutic effect of sertraline, which may be achieved by reducing suicidal ideation and improving cognitive function. Our results may provide prospective insights into the underlying pathological mechanisms in adolescents with MDD.

1. Introduction

Recently, there has been a significant increase in the prevalence of Major Depressive Disorder (MDD) during adolescence, with approximately 14% of teenagers being affected by this condition(1, 2). The World Health Organization (WHO) reports that approximately 23 million children and adolescents suffer from MDD(3). Adolescents with MDD often experience persistent symptoms that continue into adulthood, imposing a greater burden when compared to those with MDD first occurring in adulthood (4), including impaired social and academic functioning, elevated risk of physical illnesses, and substance abuse (5). Moreover, the risk of suicide among adolescents with MDD is alarmingly high, making it one of the primary causes of death in the 15-24 age group (6, 7). Nevertheless, the etiology of adolescents with MDD remains elusive.

MDD arises from the combined effects of genetic susceptibility and childhood adversity, such as abuse, neglect, and bullying(4, 5). Epigenetics refers to heritable changes in gene function without alterations in the DNA sequence, ultimately leading to changes in phenotype(6). Adolescents display greater sensitivity to epigenetic and behavioral changes triggered by stress exposure compared to adults(7). Noncoding RNA (ncRNA), especially long non-coding RNA (lncRNA) and microRNA (miRNA), significantly participate in the regulation of epigenetic modifications (6). LncRNA and mRNA can function as miRNA sponges, competing and co-binding with miRNA, forming a network termed competitive endogenous RNA (ceRNA) (8), that plays a crucial role in brain development, stress response, and neural plasticity(9).

In recent years, the emergence of extracellular vesicles, specifically exosomes, has provided a promising avenue for investigating the pathological mechanisms underlying adolescent depression. Exosomes are small (typically 40-100 nm in diameter) lipid-bound vesicles released by various cell types into the extracellular space (10) (11). Circulating exosomes play a crucial role in intercellular communication by packaging proteins, DNA, and non-coding RNAs (including lncRNA, miRNA, and mRNA) and delivering them to recipient cells(12).

Previous studies have substantiated the existence of miRNA differential expression in exosomes. For instance, exosomal let-7e, miR-145, and miR-146a exhibited varying expression patterns in patients with different treatment responses(13), while miR-335-5p and miR-1292-3p showed abnormal expression in patients with treatment-resistant depression(14). Furthermore, in comparison to patients diagnosed with anxiety disorder (AN) and attention deficit/hyperactivity disorder (ADHD), along with healthy controls, serum exosomal levels of miR-4433b-5p, miR-584-5p, miR-625-3p, and miR-432-5p were found to be downregulated in individuals with Major Depressive Disorder (MDD) (15) .

However, the relationship between the expression levels of lncRNA in exosomes and MDD is still unclear. Studies have shown differences in plasma exosome-derived lncRNA detected in autistic children and schizophrenic patients(16, 17). Our previous study found differential expression of lncRNA in patients with MDD(18). Candidate lncRNAs, GSK3βAS1, AS2, and AS3 were downregulated in patients with MDD but upregulated after treatment. GSK3βAS3 was associated with the severity of MDD and the intensity of life stress (19).

We hypothesize that there is an abnormal ceRNA network derived from exosomes in adolescent with MDD. We identified the abnormal ceRNA network and hub network in adolescent with MDD using Microarray and bioinformatics methods. We further validated the candidate regulatory axes in the cohort sample. Our study will provide potential insights for research into the pathological mechanisms of adolescent with MDD.

2. Methods

2.1 Participants

Two sets were included in this study. Ten adolescents with MDD and 10 health controls (HCs) were enrolled to perform microarray assay, while additional 64 adolescents with MDD and 30 HCs participated were collected as clinical cohort. All the patients were recruited from the psychiatric outpatient ward of the First Hospital of Shanxi Medical University, and HCs were recruited from the nearby community. The inclusion criteria for the patients were as follows: 1) age between 10-23 years; 2) meet the diagnostic criteria for MDD in DSM-V and diagnosed by at least 2 psychiatrists; 3) first-episode; 4) drug-naïve. The exclusion criteria are as follows: 1) with the severe or unstable nervous system, cardiovascular, liver, kidney, or endocrine diseases; 2) a previous diagnosis of bipolar disorder, schizophrenia, or other psychiatry disorders; 3) a history of neurological disease or traumatic brain injury; 4) alcohol or psychoactive substance dependence/abuse; 5) other circumstances that the researchers consider

inappropriate to participate in this study. The inclusion criteria for HCs were age between 10-23 years, and past or currently have no psychiatric disorders and physical diseases. The excluded criteria of HCs were the same as MDD patients. All the subjects were interviewed by Structured Clinical Interview for DSM-5 Disorders (SCID-5) before enrolling. All the subjects agreed to join the study and signed the informed consent. The Ethical Committee for Medicine of the First Hospital of Shanxi Medical University, China approved this study (ChiCTR2000039503).

2.2 Assessment of clinical characteristics

Hamilton Rating Scale for Anxiety (HAMA) was used to evaluate the severity of anxiety symptoms, the higher the total score, the more anxiety. 24-item Hamilton Rating Scale for Depression ($HAMD_{24}$) was the typical scale to assess the severity of depression symptoms, and the reductive ratio of HAMD24 total score was common used to measure treatment effect, it was calculated as ($HAMD_{24}$ total score after treatment- $HAMD_{24}$ total score at baseline)/ $HAMD_{24}$ total score at baseline×100%. The reductive ratio of the $HAMD_{24}$ total score was used to distinguish between the response group (≥50%) and the nonresponse group (<50%). Using self-reported Snaith Hamilton Pleasure Scale (SHAPS) to investigate the pleasurable experiences of participants. Cognitive function was evaluated with a Repeatable Battery for the Assessment of Neuropsychological Status (RBANS) which could quickly assess various cognitive domains, including immediate attention, visual breadth, speech function, attentional function, and delayed memory (20). The Beck Scale for Suicide Ideation (BSI) is a self-report scale to evaluate participants' suicidal ideation and risk. The first 5 items of the BSI are a screening device for suicidal ideation in the last week, and the fourth and fifth items are filter questions to assess active or passive suicidal ideations, if one of them is endorsed by subjects, they need to complete the subsequent 14 items which allow for an assessment of the possible suicide risk (21). The perceived pain was measured by Short-Form McGill Pain Questionnaire (SF-MPQ) including 3 dimensions: Pain Rating Index (PRI), 10-cm visual analog scale (VAS) for average pain, and Present Pain Intensity (PPI)(22). All participants were assessed on these scales at baseline and after 8 weeks of treatment.

2.3 Treatment

Sixty-four adolescents with MDD received sertraline treatment with an initial dose of 25mg, slowly increasing to a final dose of 100-150mg over the course of 8 weeks. Fifty-four patients adhered to the end of treatment (12 males, 42 females). The remaining 10 patients were ruled out from further study due to dropout (*n*=5), intolerance for side effects (*n*=3), or reluctance to receive any treatment (*n*=2). Benzodiazepines were unrestricted from use during the research period. In addition, a part of the patients received repetitive transcranial magnetic stimulation (rTMS) therapy (*n*=12) or psychotherapy (*n*=16).

2.4 Plasma exosomes isolation and exosomal total RNA extraction

We collected 10ml blood samples from the cubital vein per subject, and the blood samples were centrifuged at 3500rpm for 10 min immediately to obtain plasma and then frozen in the -80°C refrigerator for further use. The exoRNeasy Midi and Maxi Kits (Qiagen, Cat. NO: 77144, Germany) were used to isolate the plasma exosome and extract exosomal total RNA per the manufacturer's instruction. Briefly, the first step was to isolate the plasma exosome. 4ml pre-filtered plasma was mixed with Buffer XBP and bound to an exoEasy membrane affinity spin column. The bound exosomes are washed with 10 ml Buffer XWP. The plasma-derived exosomes were bounded in the membrane and are then ready to use in exosome total RNA extraction. The bound exosomes were lysed with QIAzol. Chloroform is added to the QIAzol eluate, and the aqueous phase is recovered and mixed with ethanol. Then the mixture was transferred to the spin column and centrifuged. Total RNA binds to the spin column, which was washed three times. The purified total RNAs were eluted with 14 µl RNase-free water. The total RNAs quantity and quality were measured by NanoDrop™ One (Thermo Fisher, ND-ONE-W, MA, USA) and then frozen in a -80°Crefrigerator for further use.

2.5 Microarray assay

The Arraystar Human LncRNA Microarray version 5.0 technology (Agilent Technologies, Santa Clara, CA, USA) enables to detect lncRNAs and mRNAs simultaneously and can detect approximately 39,317 lncRNAs and 21,174 mRNAs. Ten adolescent MDD with NSSI behavior and 10 HCs were enrolled in microarray analysis. The microarray analysis was performed at KangChen Bio-tech (Shanghai, China). The purified mRNA was obtained by removing the rRNA from the total RNA. Then, each sample was amplified and transcribed into cDNA with the labeling Cy3. The labeled probes were hybridized with the high-density microarray. After hybridization, the fluorescence intensity of the microarray was scanned with a GenePix-4000B scanner, and the results were converted to digital numbers for long-term preservation. The raw data were analyzed using Agilent feature extraction software. Differentially expressed lncRNAs (DElncRNAs) and mRNAs (DEmRNAs) between the two groups were identified with the criteria that the absolute value of log2 fold change >2.0 and FDR< 0.05. Volcano plots were generated by the R package at version 3.6.3.

The microarray data have been uploaded to the National Center for Biotechnology Information (NCBI) gene expression omnibus (GEO) database with the accession number GSE217811.

2.6 ceRNA network establishment

The top 10 up-regulated (4) and down-regulated (3) lncRNAs from the above DElncRNAs had been analyzed to match miRNAs using StarBase database (23). Targeted mRNAs of matched-miRNAs were predicted and overlapped by MiRDB(24) and TargetScan(25) databases. They overlapped with DEmRNAs

from microarray analysis. Detail flow was provided in Figure 1a. LncRNA-miRNA-mRNA ceRNA networks were generated via Cytoscape software 3.7.1 with the cytoHubba plugin.

2.7 GO function and KEGG pathway enrichment analysis

Gene Ontology (GO) is a gene function classification entry (http://www.geneontology.org), which covers three domains: Biological Process (BP), Cellular Component (CC), and Molecular Function (MF) of DEmRNAs had been analyzed. The Kyoto encyclopedia of genes and genomes (KEGG) is a database that integrates genomic, chemical, and systemic functional information to understand the biological function of genes of interest and pathways. Potential pathways of overlapped DEmRNAs were listed. Statistical analysis and visualization were performed in clusterProfiler and ggplot2 package of R version 3.6.3, *p*-value<0.05 was considered significantly different.

2.8 Quantitative reverse-transcription polymerase chain reaction (qRT-PCR)

Reverse transcription was accomplished by 2 kits. *TransScript®* Uni All-in-One First-Strand cDNA Synthesis SuperMix (TransGen Biotech, AU341, Beijing, China) was used to synthesize the cDNA of long-chain RNAs like lncRNAs and mRNAs. *TransScript®* miRNA First-Strand cDNA Synthesis Super Mix (TransGen Biotech, AT351, Beijing, China) took miRNA as a template, poly-A tailing, and cDNA synthesis were completed in the same reaction system. The experiment was carried out according to the manufacturer's instructions. The primer sequences were designed by Oligo7 software and compounded at General Biol (Shanghai, China) (see Table S1). The amplification conditions were: pre-denaturation at 94℃ for 10 min, followed by 45 cycles of denaturation at 94℃ for 5s, and annealing and extension at 60℃for the 30s. Gene expression was quantified using the software provided by the manufacturer (BIO-RAD CFX connect real-time system, #1855201, CA, USA), and analyzed according to the Standard amplification curves.

2.9 Statistical analysis

Statistical analyses were performed using SPSS v27.0 software. Data were presented as mean ± standard deviation (SD), and *p*-value < 0.05 was considered statistically significant. The test of normal distribution for quantitative data, including age, scale scores, and expression levels of lncRNAs, miRNAs, and mRNAs within candidate regulatory axes in subjects were analyzed by Shapiro–Wilk test. The parametric test was used for the normal distribution, and vice versa. Age and scale scores belonged to the normal distributions, Student's t-test was used to analyze the difference between the MDD group and the HC group at baseline, and paired t-test was performed to analyze the difference before and after treatment with the MDD group. The expression levels of lncRNAs, miRNAs, and mRNAs within candidate

regulatory axes were not subjected to the normal distributions, therefore, the Mann-Whitney U test was used to analyze the difference between HCs and MDD group at baseline, response group, and nonresponse group. Wilcoxon's signed-rank test was used to analyze the expression levels of the MDD group before and after treatment. Qualitative data, including sex, non-single child, public/private school, and family history were analyzed by Chi-squared tests. Binary logistic regression was used to explore whether lncRNAs, miRNAs, and mRNAs within candidate regulatory axes at baseline could predict the post-treatment effect. Spearman correlation was applied to investigate the relationship between the change of scale scores and the expression level changes of candidate lncRNAs, miRNAs, and mRNAs before and after treatment. In addition, receiver operating characteristics (ROC) curves and areas under the ROC curves (AUC) were used to estimate the diagnostic performance of candidate lncRNAs, miRNAs, and mRNAs. The number of AUC closed to 1.0 reflecting a better method for the prediction of the model. The best combination of sensitivity and specificity were represented by the highest Youden index.

3. Results

3.1 Demographic and clinical characteristics of adolescents with MDD & HCs

The demographic and clinical characteristics of all participants were summarized in Table S2 and S3. Firstly, no significant differences were found between microarray samples (discovery det) and validation set in age and sex. Single-child families, and public/private schools, with or without family history had no significant differences between MDD patients and healthy controls (HCs) in validation set. In addition, 25 MDD patients had suicide attempts before being recruited, and 28 patients had a good response to antidepressant treatment (HAMD decrease from baseline≥50%). The remaining 26 patients had poor treatment outcomes (HAMD decrease from baseline<50%) (see Table S2). Secondly, the scale scores were compared among HCs and MDD patients before and after treatment in validation set. The total scores of HAMA, $HAMD_{24}$, SHAPS, speech function, attentional function, delayed memory, suicide ideation and risk, and VAS were significantly different between MDD and HC groups, before and after treatment of MDD patients. The scores of PRI and PPT in the MPQ scale only displayed significant differences between the MDD group at baseline and HCs, and the immediate attention of RBANS was substantially different before and after treatment of the MDD group. No significant differences were observed in the visual breadth dimension of the RBANS between MDD and HC groups, and MDD patients before and after treatment (see Table S3).

3.2 Differential expression profiles of plasma exosomal lncRNAs and mRNAs

The easiest access to compare the difference between MDD patients and the HCs group is to analyze human blood samples, therefore, we collected blood samples from the cubital vein per subject to extract the plasma exosome. Firstly, 3752 differentially expressed (DE)lncRNAs were found between these two groups, expression of 1111 and 2641 lncRNAs were upregulated and downregulated, respectively.

Secondly, 1859 DEmRNAs were separated including 671 upregulated and 1188 downregulated mRNAs between the same two groups (see Figure 1b, 1c). Thirdly, the top 10 up and down-regulated DElncRNAs and DEmRNAs expressions were shown in Supplemental Table 4. Then, GO and KEGG enrichment analyses were conducted for narrowing the DEmRNAs. The upregulated mRNAs were mainly enriched in oxidoreductase activity, sequence-specific mRNA binding cytokine receptor binding (see Figure S2a), and pathways related to adherens junction, endocytosis, and cGMP-PKG signaling pathway (see Figure 1d). The downregulated mRNAs were mainly enriched in translation repressor activity, SMAD binding, phosphoprotein phosphatase activity (see Figure S2b), and pathways related to autophagy, primary bile acid biosynthesis, and cellular senescence (see Figure 1e). Next, we aimed to construct potential network of DElncRNA-miRNA-mRNA.

3.3 Establishment of two ceRNA networks

To explore the interactive relationship between lncRNA and its potential target genes, we performed the microarray analysis between MDD patients and HCs group, DElncRNAs matched with miRNAs using the Starbase database, miRDB, and TargetScan database to predict intersected mRNAs (see Figure 1a). 4 upregulated expressed lncRNAs had been predicted to complementary base pairing with 56 miRNAs, which were analyzed in starbase, miRDB, and TargetScan databases overlapped with DEmRNAs obtained from microarray data to predict 996 targeted mRNAs (see Figure S2a), while 3 downregulated expressed lncRNAs had been predicted to match 77 miRNAs for mutual complementary sequence, eventually to overlap 783 targeted mRNAs (see Figure S2b). 2 sets of lncRNA-miRNA-mRNA networks were constructed (see Figure 2a and 2c). Furthermore, 2 hub networks had been performed among the entire networks using Cytoscape with the cytoHubba plugin (see Figure 2b and 2d), the annotation and involved pathways of per gene in hub network was showed in Supplementary Table 5. In the hub network of upregulated lncRNAs, the ENST00000423999 (GeneSymbol: AC156455.1), miR-126-5p, AAK1(adaptor-associated protein kinase1) was chosen as candidate genes. Because AAK1 localized to neurons to mediate clathrin-dependent endocytosis (26) which was included in our top enriched pathways among all upregulated mRNAs (see Figure 1d). In addition, AAK1 was involved in Notch signaling pathway (see Table S5), which has been proven to be related to the pathogenesis of depression(27, 28). AC156455.1 and miR-126-5p formed a regulatory axis with AAK1 in the network based on bioinformatics prediction. Similarly, another predicting regulatory axis was identified in the hub network of downregulated lncRNAs, so the ENST00000449305 (GeneSymbol: CCDC-AS1)/ miR-6835-3p/CCND2 was selected as candidate regulatory axes, because CCND2 was involved in FoxO signaling pathway, Cellular senescence and Hedgehog signaling pathway (see Table S5), which were included in our top enriched pathways among all downregulated mRNAs (see Figure 1e).

3.4 The expression levels of plasma exosomal candidate regulatory axes in clinical cohort

The expression levels of plasma exosomal AC156455.1 in adolescents with MDD at baseline were significantly decreased compared to those after treatment (z=-2.580, P=0.010) and the healthy control group (z=-3.720, P<0.001) (see Figure 3a). The levels of miR-126-5p expression before treatment were significantly higher than those MDD after treatment group (z=-2.943, P=0.003), but there were no significant differences between the MDD group at baseline and the healthy control group (z=-1.771, P=0.077) (see Figure 3b). The expression levels of AAK1 were also significantly elevated in the MDD group compared to the healthy control group (z=-4.083, P<0.001), and reduced after treatment (z=-6.334, P<0.001) (see Figure 3c). The expression levels of CCDC18-AS1 and miR-6835-5p in the MDD group before treatment were significantly downregulated compared to the healthy control group (z=-3.262, P=0.001; z=-7.157, P<0.001), and then significantly elevated after 8 weeks of the treatments (z=-6.154, P<0.001; z=-4.818, P<0.001) (see Figure 3d and 3e). The CCND2 expression levels in the MDD group at baseline were significantly increased compared to the healthy control group (z=-2.268, P=0.023), and significantly decreased after 8 weeks of the antidepressant treatments (z=-2.887, P=0.004) (see Figure 3f).

To explore the relationship and interactive probability of plasma exosomal regulatory axes in distinguishing MDD patients from healthy controls, we conducted a ROC analysis to estimate the sensitivity and specificity of these genes within candidate regulatory axes. Due to the lack of significant differences in the expression levels of miR-126-5p between the MDD group and the healthy control group, it was not included in the analysis. The ROC curves and AUC values of AC156455.1, AAK1, CCDC18-AS1, miR-6835-5P, and CCND2 are shown (see Figure 4a and 4b), and the values of the 95% confidence interval (CI), sensitivity, and specificity are shown in Table S6. The results showed that these genes had poor discrimination between the MDD group and the healthy control group, except for miR-6835-5p. Therefore, we combined these genes as a combined indicator to perform ROC analysis again. The results showed that the combination of AC156455.1 and AAK1 had acceptable discrimination between the MDD group and the healthy control group (AUC=0.836, 95%CI=0.7500.921, sensitivity=0.958, specificity=0.635) (see Figure 4c). The combination of CCDC18-AS1, miR-6835-5P, and CCND2 also showed greater discrimination when using them separately (AUC=0.890, 95%CI=0.8110.969, sensitivity=0.720, specificity=0.942) (see Figure 4d).

3.5 Analysis the relationship between candidate regulatory axes and efficacy in adolescent with MDD

The response group and non-response group were divided based on the reductive ratio of $HAMD_{24}$ total scores as mentioned above. Compared to the non-response group, the expression levels of AAK1 were significantly reduced in the response group (z=-2.041, P=0.041) (see Figure 5c). The expression levels of CCDC18-AS1 (z=-2.128, P=0.033) and miR-6835-5p (z=-2.532, P=0.011) in the response group were significantly elevated compared to the non-response group (see Figure 5d and 5e). There were no significant differences in the expression levels of AC156455.1 (z=-0.925, P=0.355), miR-126-5p (z=-0.860, P=0.390), and CCND2 (z=-1.226, P=0.220) between the two groups (see Figure 5a, 5b, and 5f).

3.6 The predictive analysis of the candidate regulatory axes for efficacy

We aimed to understand whether the expression levels of candidate lncRNAs, miRNAs, and mRNAs at baseline could predict sertraline therapeutic effects using binary logistic regression. The results displayed that the levels of CCDC18AS1 (OR=7.024, 95%CI: 2.190~22.530, *P*=0.001), miR6835-5p (OR=3.734, 95%CI: 1.002~13.912, *P*=0.050), CCND2 (OR=0.371, 95%CI: 0.172~0.802, *P*=0.012) expression before treatment could predict the sertraline therapeutic effects after 8-week treatment. However, no significant predictive effects were found in the expression levels of AC156455.1, miR126-5p, and AAK1 (see Table 1).

Furthermore, we also investigated the relationship between certain clinical characteristics (depression, anxiety, anhedonia, suicidal ideation, suicidal risk, cognitive function, and pain) and the expression levels of three different genes (CCDC18-AS1, miR6835-5p, and CCND2). It suggested that the change in CCDC18-AS1 expression levels was negatively correlated with the changes in suicidal ideation (*r*=-0.416, *P*=0.006) and suicidal risk (*r*=-0.471, *P*=0.008), similarly, the change in miR6835-5p expression levels was negatively correlated with the changes in suicidal ideation (*r*=-0.386, *P*=0.015), and the change in CCND2 expression levels was negatively correlated with the changes in visual breadth (*r*=-0.800, *P*<0.001), attentional function (*r*=-0.510, *P*=0.018), however, RBANS total scores (*r*=-0.501, *P*=0.021), and positively correlated with changes in suicidal ideation(*r*=-0.484, *P*=0.001) (see Table 2). In summary, the changes in the expression levels of these genes CCDC18-AS1, miR6835-5p, and CCND2 had similar trends with various clinical indicators, they may play an important role in mediating the relationship between the changes in suicidal ideation and cognitive function.

4. Discussion

In this study, the abnormal ceRNA networks and hub networks of adolescent with MDD were constructed for the first time, candidate lncRNA-miRNA-mRNA regulatory pathways were identified within these hub networks and subsequently validated in the clinical cohort. Our findings revealed significant differential expression of candidate regulatory axes (AC156455.1/miR126-5p/AAK1 and CCDC18AS1/miR6835-5p/CCND2) between adolescent with MDD patients and HCs, and before and after treatment in adolescent with MDD patients. The combined indicators of genes in these two pathways could better distinguish adolescent MDD patients from healthy controls. Additionally, the expression levels of AAK1, CCDC18AS1 and miR6835-5p were different between the response group and the non-response group. Furthermore, baseline expression level of CCDC18-AS1, miR-6835-5p and CCND2 could predict the therapeutic effect of sertraline, which may be achieved by reducing suicidal ideation and improving cognitive function. Our findings may provide potential insights for the pathological mechanism of adolescent with MDD.

Adolescence constitutes a distinctive phase in an individual's lifespan characterized by profound transformations in brain development, sleep patterns, mental health, nutrition, education, schooling, and the implementation of parenting programs for caregivers(29). Some scholars contend that adolescence is

an essential and normative period marked by emotional disequilibrium and unpredictable behavior(30). Neurocognitive maturation, extending beyond the age of 20, challenges the conventional delineation of adolescence as solely spanning from 10 to 18 years, thus warranting an expansion to encompass ages from 10 to 24 to more accurately encapsulate the developmental trajectory of adolescents(31). Therefore, in alignment with these considerations, this study adopts an inclusion criterion of 10 to 23 years, which offers a more comprehensive exploration of the addressed concerns.

Exosomes are small vesicles that are released by cells in both normal and pathological states. They carry nucleic acids and proteins and can provide information about the health status of their source cells(32). Exosomal lncRNA and miRNA can be stably detected in circulating plasma and serum without being affected by RNase-dependent degradation(33, 34). Exosomes also can be easily isolated from various biological fluids such as plasma, serum, and urine(35), making them great candidates for studying pathological mechanisms. Previous studies have shown that serum exosomal miR-139-5p may be a potential diagnostic biomarker for MDD(36, while serum exosomal let-7e, miR-145, and miR-146a could predict antidepressant efficacy37). Overall, exosomes have great potential in the diagnosis and treatment of depression.

Starbase is a database that is typically used to decode miRNA-lncRNA, miRNA-mRNA, miRNA-ceRNA, miRNA-circRNA, miRNA-pseudogene and protein-RNA interaction networks from CLIP-Seq data(36). Although the database focuses on tumor-related ncRNA, Starbase v.20 contains approximately 10,000 miRNA-lncRNA interactions that can provide comprehensive matching miRNAs for differentially expressed lncRNAs(36). Using machine learning methods, miRDB predicts the targets of \miRNAs by analyzing thousands of miRNA-target interactions from high-throughput sequencing experiments(24). TargetScan predicts target genes using different mechanisms by searching for conserved 8mer, 7mer and 6mer sites that match each miRNA seed region to predict the target mRNAs of the miRNAs(37). To predict the target mRNAs of these miRNAs using the datasets from miRDB and TargetScan, only those mRNAs that were differentially expressed in microarray analysis were selected to narrow down the range of genes used to construct the ceRNA network. To further narrow down the range of genes used to construct the ceRNA network, we also used the CytoHubba plugin in Cytoscape software to screen out hub networks. Finally, we selected two pathways based on the functions of genes in the hub network: AC156455.1/miR126-5p/AAK1 and CCDC18AS1/miR6835-5p/CCND2.

AC156455.1, an m6A-modified and immune-associated long non-coding RNA, has not yet been found to be linked to neurological or psychiatric disorders(38). MiR-126-5p primarily functions in vascular and red blood cell generation, endothelial/leukocyte interactions, inflammation, and immune responses(39). Recent research has demonstrated that the expression of miR-126-5p is diminished following an 8-week course of psychological treatment in individuals with treatment-resistant depression (40). Another investigation additionally revealed decreased expression of miR-126-5p in plasma exosomes of bipolar disorder patients compared to healthy controls(41). Our study illustrates a reduction in miR-126-5p expression levels following treatment, aligning with prior research findings. A twin study that scrutinized the methylation patterns and transcriptome of peripheral blood mononuclear

cells in depression patients unveiled AAK1 as one of the notably distinct methylated regions linked to a lifelong history of depression(42). The AAK1 gene facilitates neurotransmitter release and recycling of synaptic vesicle proteins through its involvement in intracellular vesicle transport(43). Differential expression of the AAK1 protein was observed in the hippocampus of CUMS mice(44). Presently, AAK1 inhibitors are extensively under investigation as potential therapeutic agents for diverse neurological and psychiatric conditions, including schizophrenia, bipolar disorder, Parkinson's disease, and neuropathic pain(45). Our investigation identified, for the first time, the presence of AC156455.1, miR-126-5p, and AAK1 within plasma exosomes of depressed adolescents. The expression trends aligned with prior research findings.

Prior investigations have demonstrated an association between CCDC18-AS1 and the immune microenvironment. It exhibits a positive correlation with activated memory CD4 T cells, activated myeloid dendritic cells, neutrophils, M1 macrophages, and follicular helper T cells, while displaying a negative correlation with regulatory T cells(46) (47). miR-6835-5p has the capacity to interact with insulin-like growth factor 2 (IGF2) (48). Insulin-like growth factor 2 (IGF2) is a constituent of the insulin-like growth factor family and governs the proliferation, survival, and differentiation of diverse neuronal systems, encompassing cholinergic, dopaminergic, and serotonergic neurons(49). Decreased IGF2 levels in the hippocampus of mice subjected to CUMS are linked to heightened depressive-like behavior, a phenomenon ameliorated by augmenting IGF2 levels(50). Nonetheless, an in-depth exploration is requisite to discern the expression trend of miR-6835-5p in MDD patients and pertinent animal models. D-type cyclins (D1, D2, and D3), serving as regulatory companions of cyclin-dependent kinases 4 and 6 (CDK4 and CDK6), constitute pivotal elements propelling the progression of the cell cycle(51). CCND2 has been implicated in the etiology of schizophrenia based on antecedent research(52). Knockout mouse models deficient in CCND2 manifest hippocampal hyperactivity patterns akin to those observed in prodromal schizophrenia patients. Additionally, these models display novelty-induced hyperactivity (a rodent behavior associated with positive symptoms of schizophrenia), a preference for sucrose, compromised executive function, and deficits in working memory(53). Conversely, stress-induced depression model mice, despite exhibiting sucrose preference, impaired executive function, and compromised working memory, present diminished hippocampal activity(54). Notably, this manifestation is amenable to reversal through administration of antidepressant medication. Owing to disparate mechanisms, the function of CCND2 in the context of MDD mandates additional experimental validation. Furthermore, GSK3β has the capacity to impede the expression of CCND2(55). Earlier research conducted by our team signaled a reduction in GSK3β levels among patients afflicted with MDD(56), which is consistent with our current findings.

The top five enriched pathways of CCND2 are the FoxO signaling pathway, cell cycle regulation, p53 signaling pathway, PI3K-Akt signaling pathway, and cellular senescence. MiR-6835-5p is associated with LPS-induced inflammation and results in the dysregulation of FOXO3a expression(57). The FOXO gene family forms the central components of the FoxO signaling pathway. FOXO is likely subject to regulation by serotonin or norepinephrine signals, the hypothalamic-pituitary-adrenal (HPA) axis, and brain-derived neurotrophic factor (BDNF), all of which play a role in the onset and progression of depression(58). Earlier

studies indicate that activation of the PI3K/Akt/FoxO3a and PKA/CREB signaling pathways is intricately associated with the pathogenesis of depression and could potentially function as downstream targets of fluoxetine(59).

The present study has several limitations. Firstly, the sample size was small, particularly within the HC group, potentially giving rise to the risk of encountering false negatives. Notably, the calculated p-value of 0.77 for the differential expression of miR-126-5p between the MDD group and the HC group indicates a lack of substantial statistical significance. The pursuit of validation in a more extensive cohort may yield results of heightened accuracy. Secondly, the two candidate regulatory axes were forecasted using bioinformatics methodologies, necessitating validation of the gene's direct interactions and mutual regulatory mechanisms through subsequent cellular experiments. Thirdly, there exists an inadequate understanding of the origins and destinations of exosomes. Earlier investigations have demonstrated that exosomes derived from the blood of individuals with MDD, upon being injected into mice, exhibit a propensity to amass within the murine brain, and the mice were observed to depression-like behavior subsequently(60). This observation could potentially offer valuable insights guiding the trajectory of our forthcoming research endeavors.

In this study, we have firstly identified that abnormal plasma exosome-derived ceRNA network in adolescents with MDD. Furthermore, the candidate regulatory axes demonstrate varied expression patterns in both adolescents with MDD and HCs, both prior to and post-treatment in adolescents with MDD. Our study potentially offers a novel direction for exploring the pathological mechanisms of adolescent with MDD. However, further validation of the regulatory functions of the candidate pathways and their roles in MDD requires additional verification through animal and cellular experiments.

Declarations

Funding

This work was supported by National Natural Science Foundation of China (grant numbers 82171534, 81601193), Central Guidance on Local Science and Technology Development Fund of Shanxi Province (grant numbers YDZJSX2022A063), the special fund for Science and Technology Innovation Teams of Shanxi Province(grant numbers 202204051001027), Key Research and Development Project (International Cooperation) of Shanxi Province (grant numbers 201903D421059).

Ethics approval

All the subjects agreed to join the study and signed the informed consent. The Ethical Committee for Medicine of the First Hospital of Shanxi Medical University, China approved this study (ChiCTR2000039503).

CRediT authorship contribution statement

Yifan Xu: Conceptualization, Data curation, Data analysis, Visualization, Writing – original draft. **Rong Zhang:** Conceptualization, Data analysis, Visualization, Writing –review & editing. **Xinzhe Du and Yangxi Huang:** Experiment, Data analysis, Visualization, Writing –review & editing. **Yao Gao:** Conceptualization, Data curation, Visualization, Writing – review & editing. **Yujiao Wen and Dan Qiao:** Data curation, Visualization, Writing – review & editing. **Zhifen Liu and Ning sun:** Conceptualization, Supervision, Data curation, Visualization, Writing – review & editing.

Declaration of Competing Interest

The authors have no conflicts of interest to disclose.

Acknowledgments

We thank all the participants who have contributed to this article.

Preprint statement

This manuscript had uploaded as a preprint on Research Square with the link https://www.researchsquare.com/article/rs-2348047/v4.

Data availability statement

The microarray data have been uploaded to the National Center for Biotechnology Information (NCBI) gene expression omnibus (GEO) database with the accession number GSE217811. The clinical scales and qRT-PCR data used to support the findings of this study are available from the corresponding author upon request.

Supplementary Materials

See Table S1-S7 and Figures S1-S2 in the Supplementary Material for comprehensive analysis.

References

1. Avenevoli S, Swendsen J, He J-P, Burstein M, Merikangas KR. Major depression in the national comorbidity survey-adolescent supplement: prevalence, correlates, and treatment. J Am Acad Child Adolesc Psychiatry. 2015;54(1).

2. Cohen P, Cohen J, Kasen S, Velez C, Hartmark C, Johnson J, et al. An epidemiological study of disorders in late childhood and adolescence–I. Age- and gender-specific prevalence. Journal of child psychology and psychiatry, and allied disciplines. 1993;34(6):851-67.

3. Mental disorders 2022 [Available from: https://www.who.int/news-room/fact-sheets/detail/mental-disorders.

4. Ho TC, King LS. Mechanisms of neuroplasticity linking early adversity to depression: developmental considerations. Translational Psychiatry. 2021;11(1):517.

5. Wray NR, Ripke S, Mattheisen M, Trzaskowski M, Byrne EM, Abdellaoui A, et al. Genome-wide association analyses identify 44 risk variants and refine the genetic architecture of major depression. Nat Genet. 2018;50(5):668-81.

6. Lolak S, Suwannarat P, Lipsky RH. Epigenetics of depression. Prog Mol Biol Transl Sci. 2014;128:103-37.

7. Dion A, Muñoz PT, Franklin TB. Epigenetic mechanisms impacted by chronic stress across the rodent lifespan. Neurobiol Stress. 2022;17:100434.

8. Tay Y, Rinn J, Pandolfi PP. The multilayered complexity of ceRNA crosstalk and competition. Nature. 2014;505(7483):344-52.

9. Yoshino Y, Dwivedi Y. Non-Coding RNAs in Psychiatric Disorders and Suicidal Behavior. Front Psychiatry. 2020;11:543893.

10. Pegtel DM, Peferoen L, Amor S. Extracellular vesicles as modulators of cell-to-cell communication in the healthy and diseased brain. Philos Trans R Soc Lond B Biol Sci. 2014;369(1652).

11. Zaborowski MP, Balaj L, Breakefield XO, Lai CP. Extracellular Vesicles: Composition, Biological Relevance, and Methods of Study. Bioscience. 2015;65(8):783-97.

12. Caby MP, Lankar D, Vincendeau-Scherrer C, Raposo G, Bonnerot C. Exosomal-like vesicles are present in human blood plasma. Int Immunol. 2005;17(7):879-87.

13. Hung Y-Y, Chou C-K, Yang Y-C, Fu H-C, Loh E-W, Kang H-Y. Exosomal let-7e, miR-21-5p, miR-145, miR-146a and miR-155 in Predicting Antidepressants Response in Patients with Major Depressive Disorder. Biomedicines. 2021;9(10).

14. Li L-D, Naveed M, Du Z-W, Ding H, Gu K, Wei L-L, et al. Abnormal expression profile of plasma-derived exosomal microRNAs in patients with treatment-resistant depression. Hum Genomics. 2021;15(1):55.

15. Honorato-Mauer J, Xavier G, Ota VK, Chehimi SN, Mafra F, Cuóco C, et al. Alterations in microRNA of extracellular vesicles associated with major depression, attention-deficit/hyperactivity and anxiety disorders in adolescents. Transl Psychiatry. 2023;13(1):47.

16. Fang Y, Wan C, Wen Y, Wu Z, Pan J, Zhong M, et al. Autism-associated synaptic vesicle transcripts are differentially expressed in maternal plasma exosomes of physiopathologic pregnancies. J Transl Med. 2021;19(1):154.

17. Safari MR, Komaki A, Arsang-Jang S, Taheri M, Ghafouri-Fard S. Expression Pattern of Long Non-coding RNAs in Schizophrenic Patients. Cell Mol Neurobiol. 2019;39(2):211-21.

18. Liu Z, Li X, Sun N, Xu Y, Meng Y, Yang C, et al. Microarray profiling and co-expression network analysis of circulating lncRNAs and mRNAs associated with major depressive disorder. PloS One. 2014;9(3):e93388.

19. Liu Z, Li X, Chen C, Sun N, Wang Y, Yang C, et al. Identification of antisense lncRNAs targeting GSK3β as a regulator in major depressive disorder. Epigenomics. 2020;12(19):1725-38.

20. Shura RD, Brearly TW, Rowland JA, Martindale SL, Miskey HM, Duff K. RBANS Validity Indices: a Systematic Review and Meta-Analysis. Neuropsychol Rev. 2018;28(3):269-84.

21. Kliem S, Lohmann A, Mossle T, Brahler E. German Beck Scale for Suicide Ideation (BSS): psychometric properties from a representative population survey. BMC Psychiatry. 2017;17(1):389.

22. Hawker GA, Mian S, Kendzerska T, French M. Measures of adult pain: Visual Analog Scale for Pain (VAS Pain), Numeric Rating Scale for Pain (NRS Pain), McGill Pain Questionnaire (MPQ), Short-Form McGill Pain Questionnaire (SF-MPQ), Chronic Pain Grade Scale (CPGS), Short Form-36 Bodily Pain Scale (SF-36 BPS), and Measure of Intermittent and Constant Osteoarthritis Pain (ICOAP). Arthritis Care Res (Hoboken). 2011;63 Suppl 11:S240-52.

23. Li JH, Liu S, Zhou H, Qu LH, Yang JH. starBase v2.0: decoding miRNA-ceRNA, miRNA-ncRNA and protein-RNA interaction networks from large-scale CLIP-Seq data. Nucleic Acids Res. 2014;42(Database issue):D92-7.

24. Chen Y, Wang X. miRDB: an online database for prediction of functional microRNA targets. Nucleic Acids Res. 2020;48(D1):D127-D31.

25. Agarwal V, Bell GW, Nam JW, Bartel DP. Predicting effective microRNA target sites in mammalian mRNAs. Elife. 2015;4.

26. Tonello R, Anderson WB, Davidson S, Escriou V, Yang L, Schmidt BL, et al. The contribution of endocytosis to sensitization of nociceptors and synaptic transmission in nociceptive circuits. Pain. 2022.

27. Wang W, Li W, Wu Y, Tian X, Duan H, Li S, et al. Genome-wide DNA methylation and gene expression analyses in monozygotic twins identify potential biomarkers of depression. Transl Psychiatry. 2021;11(1):416.

28. Zhang J, Zhang N, Lei J, Jing B, Li M, Tian H, et al. Fluoxetine shows neuroprotective effects against LPS-induced neuroinflammation via the Notch signaling pathway. International immunopharmacology. 2022;113(Pt A):109417.

29. Coleman JC. The Nature of Adolescence (4th ed.): Routledge; 2010.

30. Powers SI, Hauser ST, Kilner LA. Adolescent mental health. Am Psychol. 1989;44(2):200-8.

31. Sawyer SM, Azzopardi PS, Wickremarathne D, Patton GC. The age of adolescence. Lancet Child Adolesc Health. 2018;2(3):223-8.

32. Pant S, Hilton H, Burczynski ME. The multifaceted exosome: biogenesis, role in normal and aberrant cellular function, and frontiers for pharmacological and biomarker opportunities. Biochem Pharmacol. 2012;83(11):1484-94.

33. Mitchell PS, Parkin RK, Kroh EM, Fritz BR, Wyman SK, Pogosova-Agadjanyan EL, et al. Circulating microRNAs as stable blood-based markers for cancer detection. Proceedings of the National Academy of Sciences of the United States of America. 2008;105(30):10513-8.

34. Li Q, Shao Y, Zhang X, Zheng T, Miao M, Qin L, et al. Plasma long noncoding RNA protected by exosomes as a potential stable biomarker for gastric cancer. Tumour Biol. 2015;36(3):2007-12.

35. Lin J, Li J, Huang B, Liu J, Chen X, Chen X-M, et al. Exosomes: novel biomarkers for clinical diagnosis. ScientificWorldJournal. 2015;2015:657086.

36. Li J-H, Liu S, Zhou H, Qu L-H, Yang J-H. starBase v2.0: decoding miRNA-ceRNA, miRNA-ncRNA and protein-RNA interaction networks from large-scale CLIP-Seq data. Nucleic Acids Research. 2014;42(Database issue):D92-D7.

37. Lewis BP, Burge CB, Bartel DP. Conserved seed pairing, often flanked by adenosines, indicates that thousands of human genes are microRNA targets. Cell. 2005;120(1):15-20.

38. Yuan C, Liu C, Zhao S, Zhang X, Jia H, Chen B, et al. The Role of N6-Methyladenosine-Associated lncRNAs in the Immune Microenvironment and Prognosis of Colorectal Cancer. J Oncol. 2022;2022:4689396.

39. Sonntag KC, Woo T-UW, Krichevsky AM. Converging miRNA functions in diverse brain disorders: a case for miR-124 and miR-126. Exp Neurol. 2012;235(2):427-35.

40. Maffioletti E, Bocchio-Chiavetto L, Perusi G, Carvalho Silva R, Sacco C, Bazzanella R, et al. Inflammation-related microRNAs are involved in stressful life events exposure and in trauma-focused psychotherapy in treatment-resistant depressed patients. Eur J Psychotraumatol. 2021;12(1):1987655.

41. Ceylan D, Tufekci KU, Keskinoglu P, Genc S, Özerdem A. Circulating exosomal microRNAs in bipolar disorder. Journal of Affective Disorders. 2020;262.

42. Zhu Y, Strachan E, Fowler E, Bacus T, Roy-Byrne P, Zhao J. Genome-wide profiling of DNA methylome and transcriptome in peripheral blood monocytes for major depression: A Monozygotic Discordant Twin Study. Translational Psychiatry. 2019;9(1):215.

43. Nakazawa T, Hashimoto R, Sakoori K, Sugaya Y, Tanimura A, Hashimotodani Y, et al. Emerging roles of ARHGAP33 in intracellular trafficking of TrkB and pathophysiology of neuropsychiatric disorders. Nat Commun. 2016;7:10594.

44. Han X, Shao W, Liu Z, Fan S, Yu J, Chen J, et al. iTRAQ-based quantitative analysis of hippocampal postsynaptic density-associated proteins in a rat chronic mild stress model of depression. Neuroscience. 2015;298:220-92.

45. Martinez-Gualda B, Schols D, De Jonghe S. A patent review of adaptor associated kinase 1 (AAK1) inhibitors (2013-present). Expert Opin Ther Pat. 2021;31(10):911-36.

46. Xia F, Yan Y, Shen C. A Prognostic Pyroptosis-Related lncRNAs Risk Model Correlates With the Immune Microenvironment in Colon Adenocarcinoma. Front Cell Dev Biol. 2021;9:811734.

47. Fan F, Huang Z, Chen Y. Integrated analysis of immune-related long noncoding RNAs as diagnostic biomarkers in psoriasis. PeerJ. 2021;9:e11018.

48. Tang D, Wang B, Khodahemmati S, Li J, Zhou Z, Gao J, et al. A transcriptomic analysis of malignant transformation of human embryonic esophageal epithelial cells by HPV18 E6E7. Transl Cancer Res. 2020;9(3):1818-32.

49. Estil les E, Tellez N, Escoriza J, Montanya E. Increased beta-cell replication and beta-cell mass regeneration in syngeneically transplanted rat islets overexpressing insulin-like growth factor II. Cell Transplant. 2012;21(10):2119-29.

50. Luo YW, Xu Y, Cao WY, Zhong XL, Duan J, Wang XQ, et al. Insulin-like growth factor 2 mitigates depressive behavior in a rat model of chronic stress. Neuropharmacology. 2015;89:318-24.

51. Ding ZY, Li R, Zhang QJ, Wang Y, Jiang Y, Meng QY, et al. Prognostic role of cyclin D2/D3 in multiple human malignant neoplasms: A systematic review and meta-analysis. Cancer Med.

2019;8(6):2717-29.

52. Hansen T, Olsen L, Lindow M, Jakobsen KD, Ullum H, Jonsson E, et al. Brain expressed microRNAs implicated in schizophrenia etiology. PLoS One. 2007;2(9):e873.

53. Grimm CM, Aksamaz S, Schulz S, Teutsch J, Sicinski P, Liss B, et al. Schizophrenia-related cognitive dysfunction in the Cyclin-D2 knockout mouse model of ventral hippocampal hyperactivity. Transl Psychiatry. 2018;8(1):212.

54. Mahar I, Bambico FR, Mechawar N, Nobrega JN. Stress, serotonin, and hippocampal neurogenesis in relation to depression and antidepressant effects. Neurosci Biobehav Rev. 2014;38:173-92.

55. Huang W, Chang HY, Fei T, Wu H, Chen YG. GSK3 beta mediates suppression of cyclin D2 expression by tumor suppressor PTEN. Oncogene. 2007;26(17):2471-82.

56. <Identification of antisense lncRNAs.pdf>.

57. Ali T, Rahman SU, Hao Q, Li W, Liu Z, Ali Shah F, et al. Melatonin prevents neuroinflammation and relieves depression by attenuating autophagy impairment through FOXO3a regulation. J Pineal Res. 2020;69(2):e12667.

58. Rana T, Behl T, Sehgal A, Mehta V, Singh S, Sharma N, et al. Elucidating the Possible Role of FoxO in Depression. Neurochem Res. 2021;46(11):2761-75.

59. Zeng B, Li Y, Niu B, Wang X, Cheng Y, Zhou Z, et al. Involvement of PI3K/Akt/FoxO3a and PKA/CREB Signaling Pathways in the Protective Effect of Fluoxetine Against Corticosterone-Induced Cytotoxicity in PC12 Cells. J Mol Neurosci. 2016;59(4):567-78.

60. Wei Z-X, Xie G-J, Mao X, Zou X-P, Liao Y-J, Liu Q-S, et al. Exosomes from patients with major depression cause depressive-like behaviors in mice with involvement of miR-139-5p-regulated neurogenesis. Neuropsychopharmacology. 2020;45(6):1050-8.

Tables

Table 1. The predictive Analysis of the candidate regulatory axes for therapeutic effects

	β	SEM	*P*-value	OR	95%CI
AC156455.1	-0.161	0.522	0.758	0.852	0.306~2.370
miR126-5p	-0.222	0.207	0.282	0.801	0.534~1.200
AAK1	-0.356	0.491	0.468	0.700	0.268~1.834
CCDC18-AS1	1.9494	0.595	0.001*	7.024	2.190~22.530
MiR6835-5p	1.317	0.617	0.050*	3.734	1.002~13.912
CCND2	-0.991	0.393	0.012*	0.371	0.172~0.802

* represents P<0.05, ** represents P<0.001.

Table 2. The correlation analysis between the changes of gene expression and the changes of clinical characteristics before and after treatment.

					RBANS						BSI		SF-MPQ		
		HAMA	HAMD	SHAPS	Immediate memory	Visual breadth	Speech function	Attentional function	Delayed memory	Total score	Suicidal ideation	Suicidal risk	PRI	VAS	PPT
CCDC18-AS1	r	-0.290	-0.278	0.013	0.005	0.004	0.190	0.223	-0.293	0.004	**-0.416***	**-0.471***	-0.092	-0.245	-0.058
	P-value	0.056	0.078	0.938	0.983	0.986	0.437	0.360	0.223	0.986	**0.006**	**0.008**	0.599	0.156	0.740
miR6835	r	-0.183	-0.073	0.124	-0.174	0.260	-0.231	0.154	-0.351	-0.150	**-0.386***	-0.016	0.010	-0.064	-0.061
	P-value	0.253	0.645	0.464	0.534	0.350	0.408	0.584	0.199	0.593	**0.015**	0.938	0.955	0.726	0.739
CCND2	r	0.026	-0.179	-0.136	-0.288	**-0.800****	0.133	**-0.510***	-0.120	**-0.501***	**0.484****	0.174	-0.297	-0.173	-0.295
	P-value	0.866	0.262	0.406	0.206	**<0.001**	0.567	**0.018**	0.603	**0.021**	**0.001**	0.357	0.088	0.327	0.091

* represents P<0.05, ** represents P<0.001.

Figures

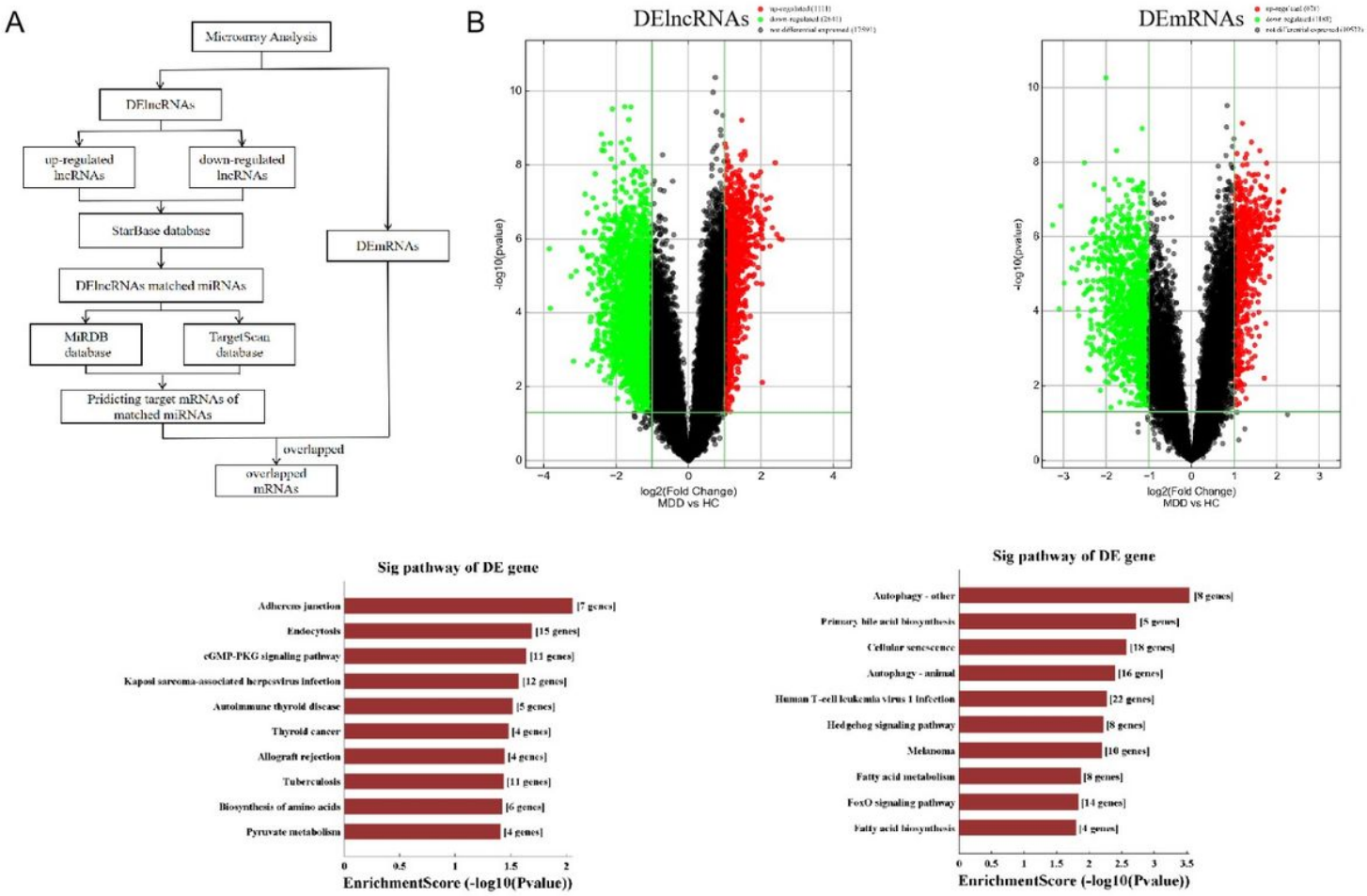

Figure 1

Differential gene expressions (DEGs) of lncRNAs, mRNAs, and enriched pathways

(A)Schematic picture of screening miRNAs and mRNAs between MDD patients and HCs group from the plasma exosome. (B)The volcano plot of DElncRNAs. Green/red dots represent down or up-regulated lncRNAs, respectively. None differentially expressed lncRNAs were displayed as black dots. (C)The volcano plot of DEmRNAs. Green/red dots represent down or up-regulated mRNAs, and black dots represent the mRNAs that were not differentially expressed between adolescent MDD and healthy controls. (D)Significant enriched pathways of up-regulated DEmRNAs. (E) Significant enriched pathways of down-regulated DEmRNAs.

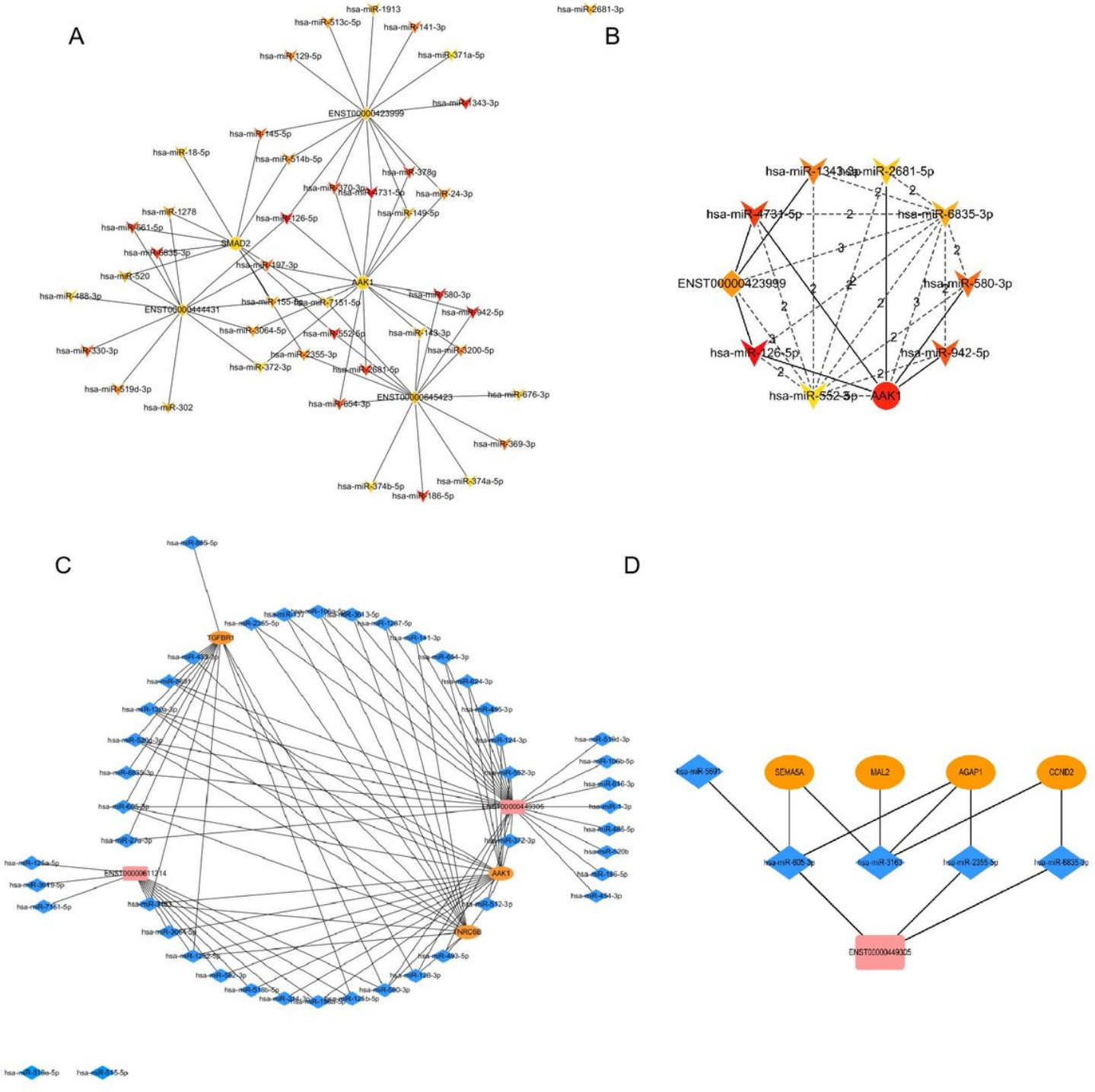

Figure 2

Establishment of Two lncRNA-miRNA-mRNA Networks and Hub-network

(A) Upregulated lncRNAs-mRNAs network. (B) Hub gene-miRNAs-lncRNAs network. (C) Downregulated lncRNAs-mRNAs network. (D) Hub gene-miRNAs-lncRNAs network. The upregulated lncRNAs are represented by orange nodes, miRNAs are represented by the yellow arrow, and mRNAs are represented by the red arrow, while the downregulated lncRNAs are represented by a pink rectangle, miRNAs are

represented by blue rhombus, and mRNAs are represented by an orange ellipse. The lines connecting the nodes represent the predicted binding between the lncRNA and miRNA or between the miRNA and mRNA.

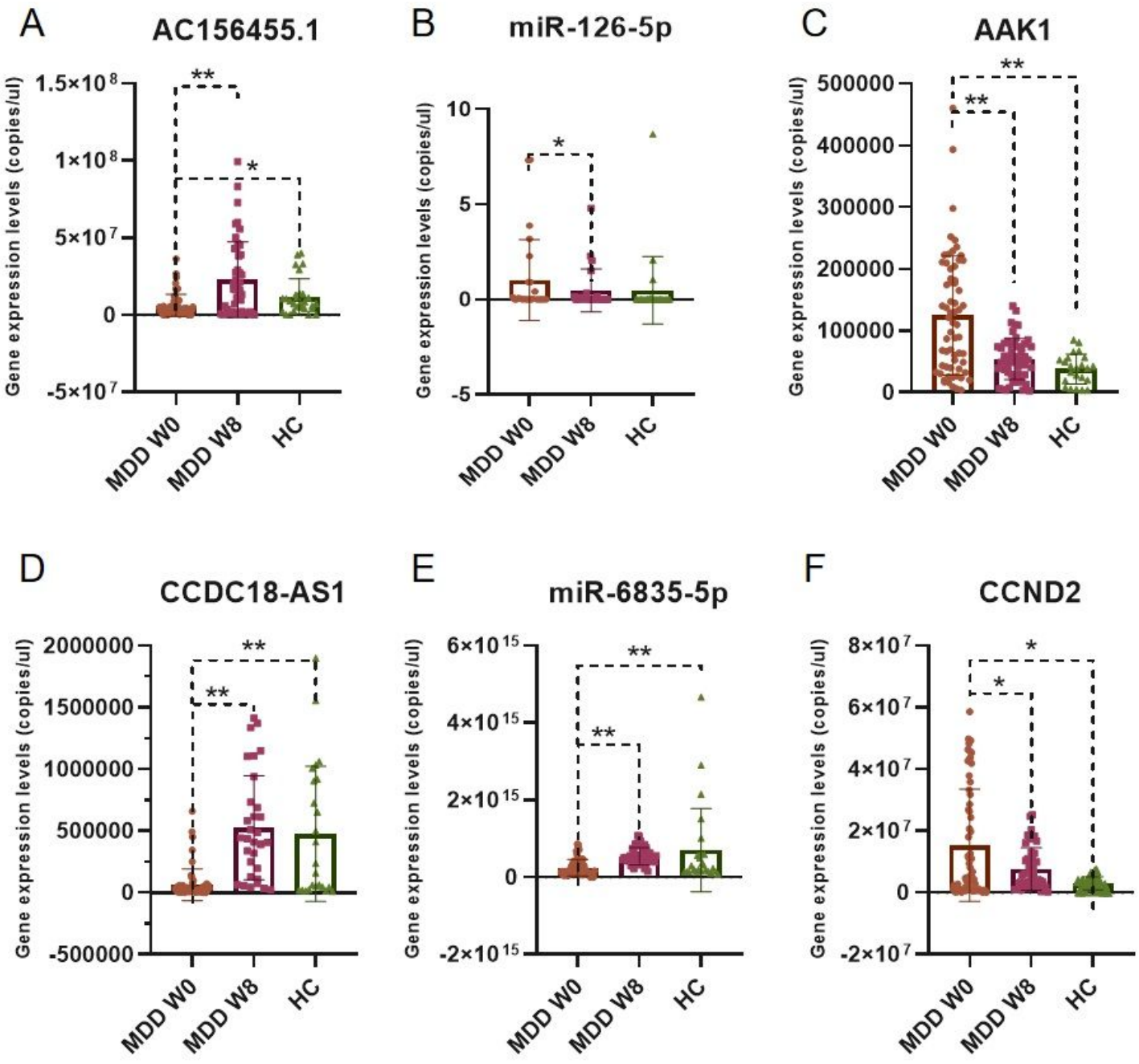

Figure 3

Differential Expressed Candidate Regulatory Axes in Clinical Cohort

(A) The comparisons of AC156455.1 expression levels between HC group and MDD group, and MDD group before and after treatment; (B) The differential expression of miR-126-5p; (C) The differential expression of AAK1; (D)(E)(F) The differential expression of CCDC18-AS1, miR-6835-5p and CCND2. * represents P<0.05, ** represents P<0.001.

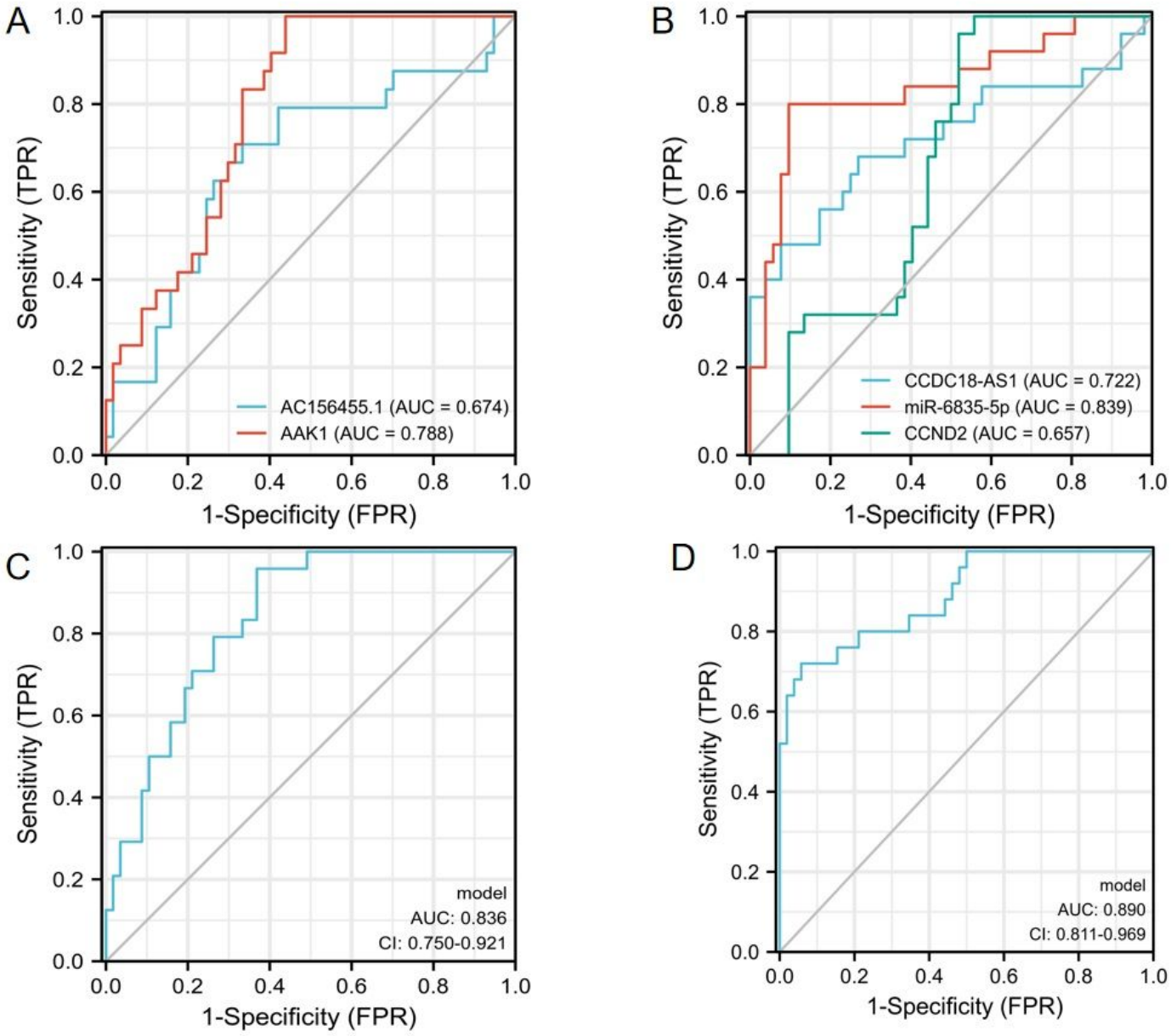

Figure 4

ROC Analysis of The Candidate Regulatory Axes

(A) ROC curves of individual AC156455.1 (blue line) and AAK1 (red line); (B) ROC curves of individual CCDC18-AS1 (blue line), miR-6835-5p (red line) and CCND2 (green line); (C) ROC curves of combined AC156455.1 and AAK1; (D) ROC curves of combined CCDC18-AS1, miR-6835-5p and CCND2.

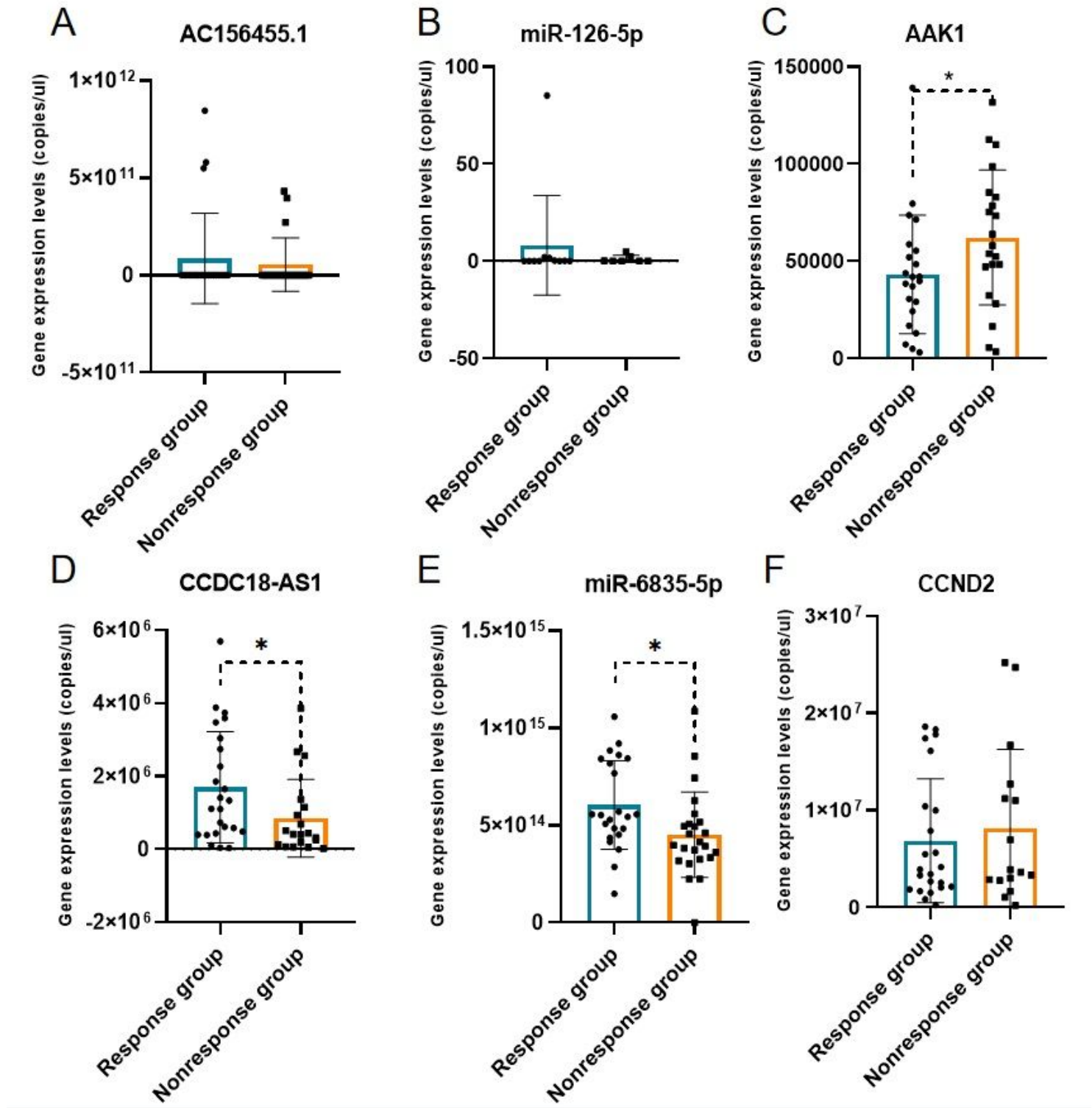

Figure 5

Comparison of Gene Expression Levels between Response Group and Nonresponse Group After Treatment.

The expression levels of (A) AC156455.1, (B) miR-126-5p, (C) AAK1, (D) CCDC18-AS1, (E) miR-6835-5p, and (F) CCND2 were measured by RT-qPCR. The x-axis represents the groups, the y-axis represents the

expression levels of genes. Data are presented as mean ± SD. **P < 0.01; *P < 0.05.

Supplementary Files

This is a list of supplementary files associated with this preprint. Click to download.

- supplementarymaterials.docx